Q. J. R. Meteorol. Soc. (1987), **113**, pp. 1193–1215 551.594.252:551.574.13:551.578.71

The influence of diffusional growth rates on the charge transfer accompanying rebounding collisions between ice crystals and soft hailstones

By B. BAKER, M. B. BAKER

Department of Geophysics, University of Washington, Seattle, U.S.A.

and

E. R. JAYARATNE*, J. LATHAM, C. P. R. SAUNDERS

Department of Pure and Applied Physics, University of Manchester Institute of Science and Technology

(Received 13 May 1986; revised 27 January 1987)

SUMMARY

Laboratory experiments designed to investigate the charge transfer accompanying rebounding collisions between ice crystals and soft hailstones were performed inside a cold room. They constitute an extension of those conducted with the same apparatus, reported in 1983 by Jayaratne *et al.* In particular, the range of temperature was extended (to cover −1·5°C to −35°C) and specific tests were performed in an effort to establish relationships between the sign and magnitude of the charging and the growth characteristics of both types of hydrometeor.

Significant charging was obtained only when the interacting surfaces were growing by vapour diffusion. The sign of the current, I, flowing to the simulated soft hailstone target in these circumstances was a sensitive function of time, liquid water content, and temperature. The complete set of results is qualitatively consistent with the hypothesis that I is positive if the target surface is growing more rapidly from the vapour than the ice crystals and is negative for the opposite case. In formulating a qualitative model of this hypothesis, account is taken of the contribution made to the diffusional growth of the target by the flux of vapour from droplets freezing onto its surface.

Crude calculations designed to assess the implications of these studies with respect to thunderstorm electrification, yield the conclusion that negative soft hailstone charging is likely to predominate over positive in most circumstances.

1. INTRODUCTION

Observational evidence on thunderstorm electrification, obtained using ground-based and airborne techniques (for example Gaskell *et al.* 1978; Krehbiel *et al.* 1979, 1983; Lhermitte and Krehbiel 1979; Christian *et al.* 1980), strongly suggests that the development of the electric field is associated with a non-inductive charging mechanism involving rebounding collisions between soft hailstones (graupel) and ice crystals (Latham 1981; Illingworth 1985). The results of laboratory experiments (for example, Reynolds *et al.* 1957; Takahashi 1978; Hallett and Saunders 1979), point to an effective process of charge transfer when the colliding ice hydrometeors coexist with supercooled water. This charge transfer process is sufficiently powerful to explain the electrification of thunderstorms, according to the calculations of Illingworth and Latham (1977) and Rawlins (1982). The mechanism of charge transfer has not been identified; various processes (for example, the thermoelectric effect (Brook 1958; Latham and Mason 1961), freezing potentials (Workman and Reynolds 1948)) have been found to be inconsistent with the experimental evidence.

A comprehensive laboratory simulation of this ice crystal/soft hailstone/riming electrification process was performed by Jayaratne *et al.* (1983), who found that the magnitude and/or sign of the charge transfer resulting from rebounding collisions between these two types of hydrometeor depended sensitively on temperature, ice crystal size, impact velocity, liquid water content of the supercooled cloud, and chemical constitution of the cloud water. These experiments underline the conclusion emanating from earlier studies that the charge transfer is greatest when hailstone/ice crystal collisions occur *in*

* Present address: Department of Physics, University of Botswana.

the presence of supercooled water which is accreted by the growing hailstone. The charge transferred in this situation is about three orders of magnitude greater than when supercooled water is absent.

In section 2 we describe some laboratory experiments which follow from those of Jayaratne *et al.* Their results permit us to define the conditions under which ice crystal/soft hailstone collisions are accompanied by significant charge transfer, and to specify the relationships between the sign of the charge transfer and the experimental parameters.

In section 3 we show that the results of all these experiments are explicable in terms of the hypothesis that the magnitude of charge transfer associated with crystal/soft hailstone collisions is appreciable only if both types of hydrometeor are growing efficiently from the vapour, and that the *sign* of the charge transfer is governed by their relative diffusional growth rates. A simple expression for the difference in these rates includes a contribution to soft hailstone growth from vapour transported laterally from accreted supercooled droplets as they freeze.

In section 4 we describe experiments designed to subject our hypothesis to further tests, and show that it is able to explain the results obtained.

In section 5 we discuss the limitations of our hypothesis and attempt to assess the implications of the collisional charging process for the electrification of thunderstorms.

Appendix A presents calculations of the diffusional growth of riming soft hailstones and the freezing times of droplets on the riming surface.

2. Laboratory experiments on ice crystal/soft hailstone charging

The laboratory experiments of Jayaratne *et al.* (1983) were repeated under more rigorously controlled conditions, with the temperature range extended down to −35 °C. The experimental procedures were basically identical to those employed by Jayaratne *et al.* and will not be described in detail here. A supercooled droplet cloud was seeded at time $t = 0$ by inserting a wire which had been chilled in liquid nitrogen. The ice crystals so produced grew by vapour diffusion, at the expense of the droplets, and the liquid water content diminished to a minimum value about one minute after seeding, and then gradually increased as crystals fell out of the cloud. The steam production rate was adjusted from run to run so that A, the average rate of deposition of rime by accretion onto a moving ice-coated metal target rod—simulating a soft hailstone—was constant. With a rod of diameter 5 mm and speed $U = 3{\cdot}0\,\mathrm{m\,s^{-1}}$, and initial liquid water content $L = 2\,\mathrm{g\,m^{-3}}$, A was approximately 3 mg min^{-1} per centimetre of rod. Continuous measurements were made of the charging current I to the target moving through this generally mixed-phase cloud.

As in the original measurements, $I = 0$ when ice crystals were absent from the cloud. Immediately after seeding, an initial positive current excursion was generally noted. Subsequent variations in I were strongly dependent on temperature. The current/time (I/t) relationships obtained for five temperatures between −1·5 °C and −35 °C are displayed in Fig. 1. It is seen that they are consistent with those obtained for the more limited temperature range covered by Jayaratne *et al.* A characteristic feature of the I/t curves when negative charging of the hailstone occurred is the fairly constant value of charging current about one minute after seeding, which corresponds approximately to the time at which L achieved its minimum value. This feature is seen in each case to be about one minute earlier than that at which I reached its maximum negative value. The reasons for this time delay, and the positive peak in I immediately following seeding, are discussed in sections 3 and 4.

The arrow displayed on each curve of Fig. 1 is the 'reference stage', defined by

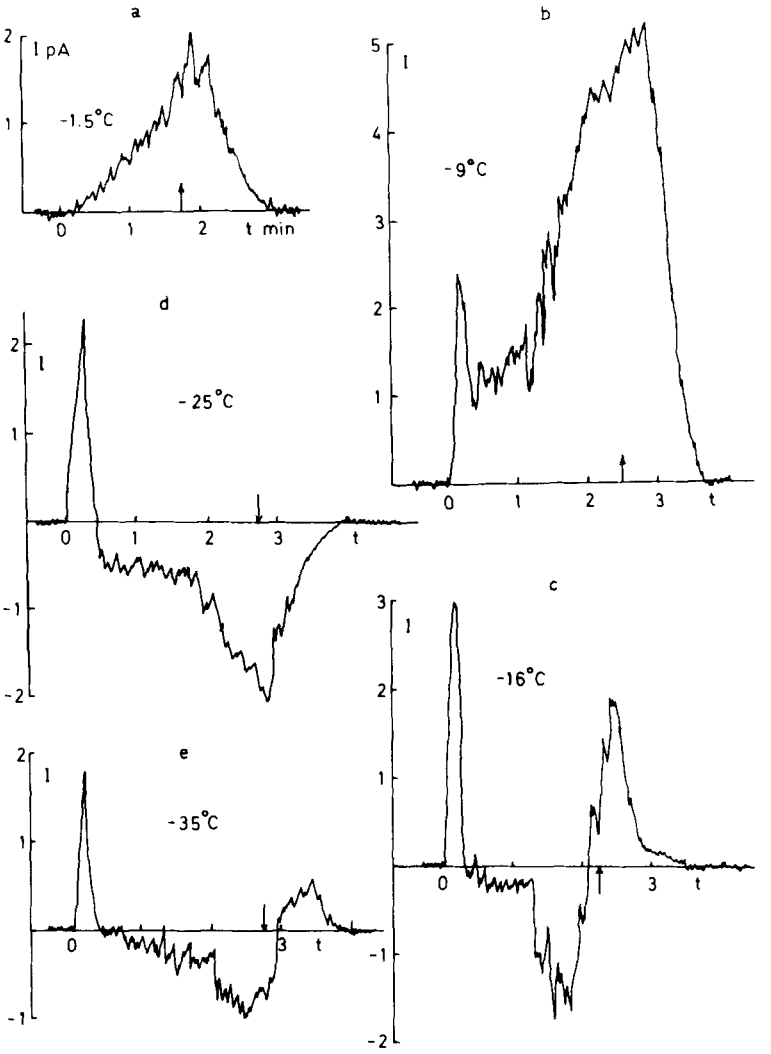

Figure 1. The charging current I to the target as a function of time t at five temperatures. The reference stage is marked by arrows. $U = 3\,\mathrm{m\,s^{-1}}$. $L = 2\,\mathrm{g\,m^{-3}}$ before seeding.

Jayaratne *et al.* as the time at which droplets re-emerge, as perceived visually, following their disappearance in the early stages of glaciation. Since the microphysical characteristics of the cloud were found to be approximately the same, at this stage, for all temperatures (typically $L \sim 0{\cdot}25\,\mathrm{g\,m^{-3}}$, ice crystal concentration $n \sim 50\,\mathrm{cm^{-3}}$, mean crystal maximum dimension $d \sim 40\,\mu\mathrm{m}$) the corresponding values of I were used in order to produce the current/temperature curve presented in Fig. 2. The general pattern of positive charging at higher temperatures and negative at lower is consistent with that found by Jayaratne *et al.* The temperature at which the sign of charging reversed is seen to be about $-18\,^{\circ}\mathrm{C}$. The diminution in I as the temperature rises above $-8\,^{\circ}\mathrm{C}$ is probably a consequence of the observed greater propensity of the crystals to adhere to the rod on impact. At temperatures lower than about $-28\,^{\circ}\mathrm{C}$, which were not achieved in the earlier experiments, the magnitude of I diminishes, but is still negative at $-35\,^{\circ}\mathrm{C}$.

The thin-wire technique developed by Jayaratne (1981) was employed to estimate the event probability, E, which is the fraction of ice crystals in the direct path of the

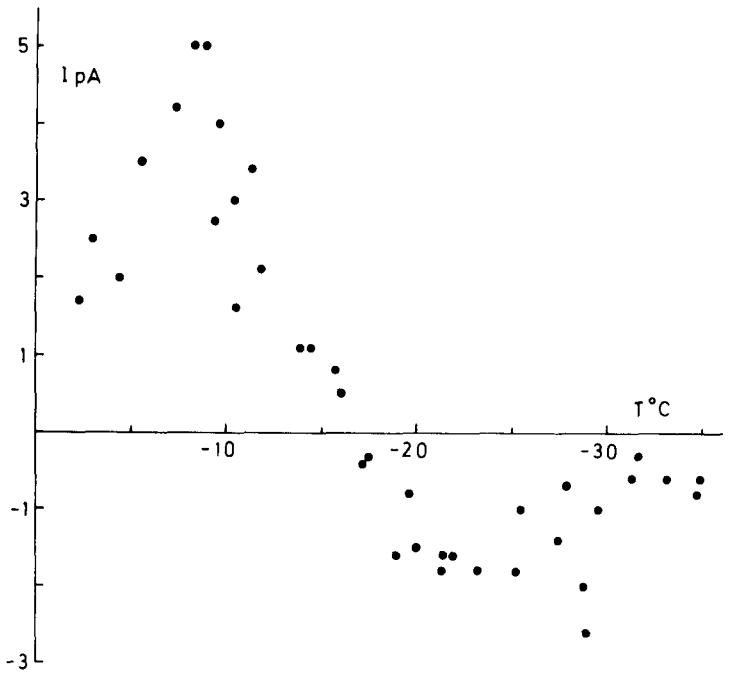

Figure 2. The charging current I to the target as a function of temperature T at the reference stage. $U = 3\,\mathrm{m\,s^{-1}}$. $L \approx 0{\cdot}3\,\mathrm{g\,m^{-3}}$. $d \approx 40\,\mu\mathrm{m}$. $n \approx 50\,\mathrm{ml^{-1}}$.

moving target which rebound from it and thus engage in separation of charge. An upper limit of $E \sim 0{\cdot}05$ was determined for the reference stage, from which, together with a knowledge of n, it was calculated that a charging current $I \sim 1$ pA (a characteristic value for the reference stage) corresponds to a charge transfer per rebounding event of $q > 0{\cdot}05$ fC. The much larger values of I observed towards the end of each run correspond to $q > 2$ fC, the increase being primarily associated with the increase in ice crystal size.

The time-development of the electrical parameters I and q, and the microphysical variables n, d and L—obtained by integrating over the measured droplet size distribution—are displayed in Fig. 3 for a characteristic run at $T = -10\,^{\circ}\mathrm{C}$.

The relationship between charging and liquid water content was examined in a series of experiments conducted at a fixed temperature. It was found that if the droplet supply was switched off in the course of a run in which the target was charging positively, I reversed sign as L diminished, and then became zero as the supply of liquid water was exhausted. This behaviour was most clearly identifiable around the reversal temperature. Figure 4 reveals the general I/A relationship observed for fixed values of U and d at $-24\,^{\circ}\mathrm{C}$. As A (and hence L) increases monotonically from zero, I increases negatively, passes through a maximum, decreases, becomes positive and continues to increase. At somewhat higher temperatures, where the charging current is always positive, I increased with increasing L. The reversal temperature was higher for lower values of L. These two latter findings were reported by Jayaratne *et al.*

No charging was observed in these experiments if droplets were absent from the cloud. We note that Jayaratne *et al.*, in an experimental arrangement in which crystals flowed past a stationary target at speeds considerably in excess of our ceiling figure of $3\,\mathrm{m\,s^{-1}}$, found very weak charging in the absence of droplets: three orders of magnitude less than in the mixed-phase case.

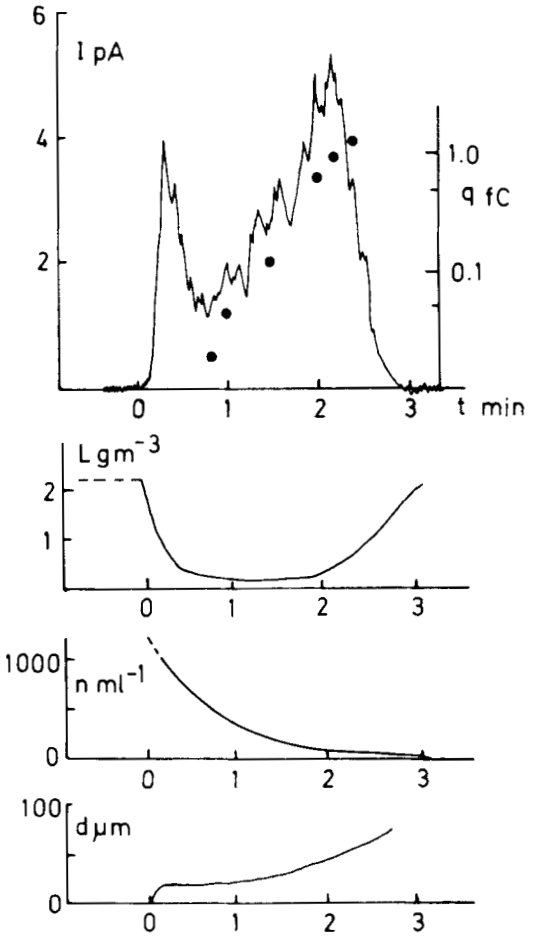

Figure 3. The temporal development of the charging current to the target I, the charge per event q, and the microphysical characteristics of the cloud during a typical run with the large nozzle at $-10°C$. $U \simeq 3\,m\,s^{-1}$. The reference stage occurred close to $t = 2$ min. The liquid water content L was derived from the integrated droplet spectrum. d and n are crystal size and concentration respectively.

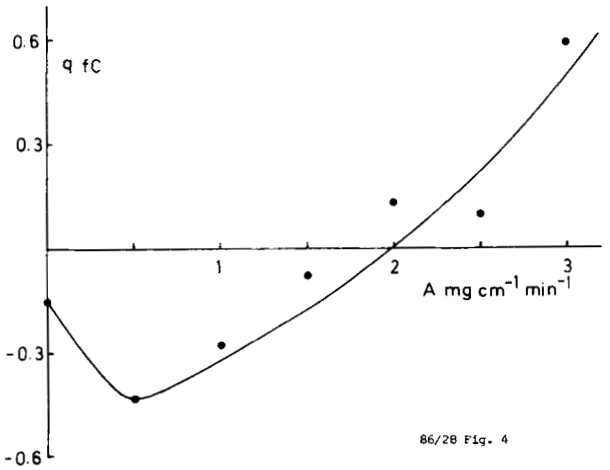

Figure 4. Average values of the charge per event q as a function of the rime accretion rate per unit length of rod, A. $T = -24 \pm 2°C$. $U = 3\,m\,s^{-1}$. $D = 50 \pm 10\,\mu m$.

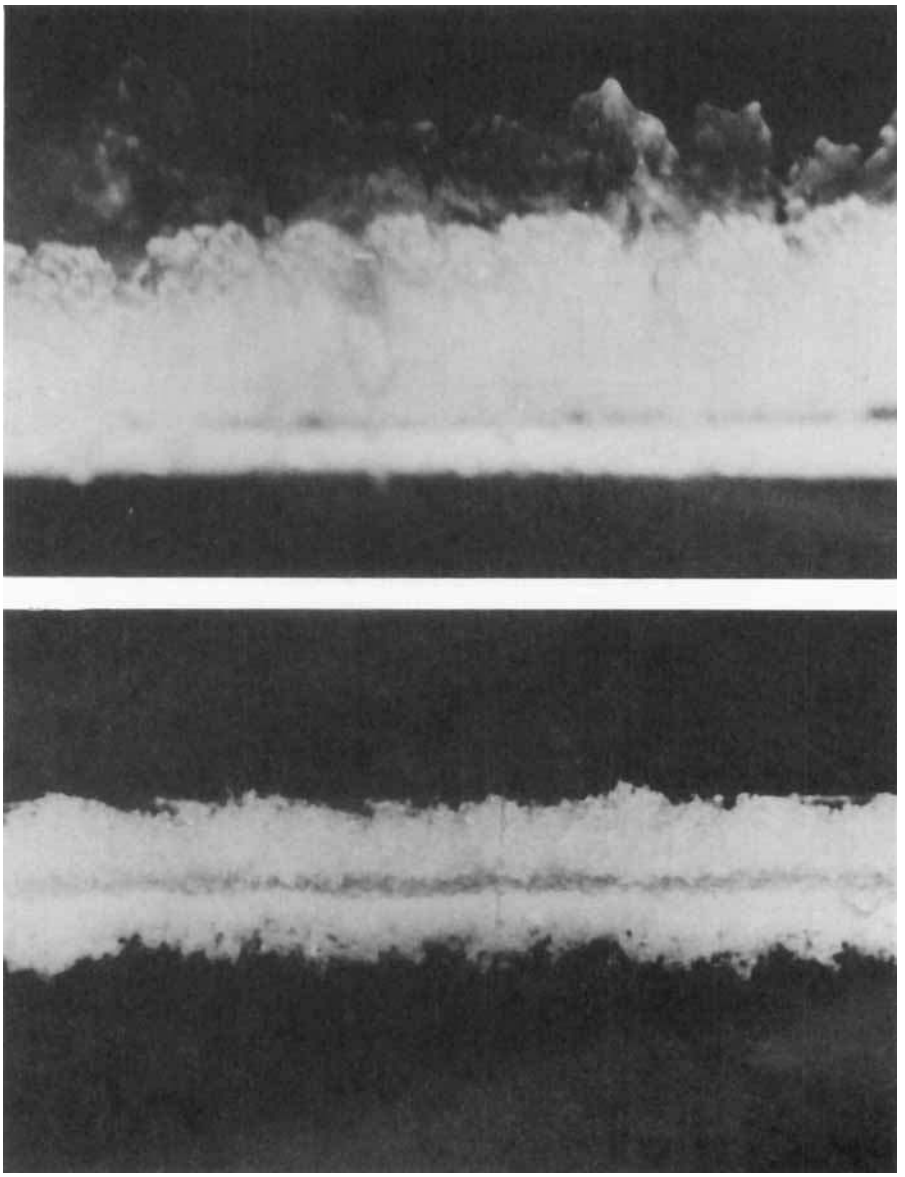

Figure 5. The 'twin-band effect', showing two distinct rime bands. $T = -15°C$. $U = 3\,m\,s^{-1}$. $L \simeq 0{\cdot}5\,g\,m^{-3}$. Top: side view of rime on target. Bottom: front view of twin bands.

Figure 5 shows a photographic close-up of the moving target; the rime has been deposited in two distinct bands, non-uniformly across the leading face of the rod. This point is mentioned again in section 5.

Jayaratne and Saunders (1985) employed a technique developed by Mossop (1984) in order to produce clouds of supercooled droplets of much smaller sizes ($<6\,\mu m$ diameter) than those utilized in the main experiments. Such droplets are too small to be collected by the rotating rod. In these circumstances the target charged negatively at $-10\,°C$ for all values of L, in direct contrast to the positive charging observed with the larger droplets at this temperature (Fig. 1(b)). The magnitude of the charging was similar to that measured in a mixed-phase cloud in the larger-droplet experiments, and two

to three orders of magnitude greater than that measured in a water-undersaturated environment by Jayaratne *et al.* and by Buser and Aufdermaur (1977). Jayaratne and Saunders pointed out that in the small-droplet experiments the ice crystals would have been growing efficiently from the vapour, whereas in the droplet-free experiments—where the charging was drastically reduced—they would not. They suggested that the surface state of the crystals exercised a controlling influence over the charging. Support for this argument was provided by further small-droplet experiments in which it was found that I dropped to undetectable values if the droplet supply was switched off in the course of a run: the maximum current with the droplets present was three orders of magnitude above the detectable limit.

In order to facilitate assessment of these various experiments in the light of the hypothesis to be developed in the subsequent section we now summarize the most important results:

(1) significant charging of the simulated soft hailstone target occurs only when it is moving through a mixed-phase cloud; the charging results from rebounding collisions between ice crystals and the target;

(2) significant charging requires water saturation, but not necessarily riming, so that the target and the ice crystals are growing from the vapour;

(3) the target charge tends to be positive at higher temperatures and negative at lower temperatures;

(4) the most pronounced effects of increasing the liquid water content are to make I more positive and to shift the reversal temperature to lower values.

In section 3 we consider these points, together with the more detailed ones described in this section, and endeavour to explain the set of I/t curves presented in Fig. 1.

3. Development and first assessment of the hypothesis

The experiments described in section 2 reveal that significant charging occurs only when the soft hailstone target and the ice crystals with which it collides are both growing from the vapour. We now assume that the *sign* of the charging is determined by the relative diffusional growth rates of the colliding hydrometeors; i.e. that the target becomes positively charged if it is growing more quickly by vapour diffusion than the ice crystals, and negatively charged if it is growing more slowly. This hypothesis embodies no physical mechanism—the charge transfer may be governed by any parameter which varies in a similar manner to the relative diffusional growth rate—but for the moment we enquire whether it is capable of explaining the results presented in section 2. We define the parameter S as the difference between these diffusional growth rates (soft hailstone minus crystals). According to our hypothesis I and S have the same sign.

The target and the crystals grow efficiently from the vapour only when water droplets exist within the cloud. The droplets act as deep-field sources of water vapour, and the diffusional growth rates of the target and crystals from the field may be expressed approximately as $K_1F_1(\rho_W - \rho_I)/R$ and $K_2F_2(\rho_W - \rho_I)/d$, where K_1 and K_2 are constants which embody factors such as the diffusion coefficient, the surface structure of the hailstone, the effective location of the vapour source, the shape of the ice crystals etc., F_1 and F_2 are ventilation coefficients, ρ_W is the saturation vapour density with respect to water at the temperature T in question, ρ_I the corresponding saturation vapour density with respect to ice, and R and d respectively are the target radius and the size of a crystal which collides with it.

On the basis of these two deep-field terms only, S and therefore the sign of charging of the target would always be negative, since $d/R \ll 1$. However, when the target is

accreting supercooled droplets, there is an additional contribution to the vapour growth rate of the hailstone, namely the diffusion of water vapour from each droplet to the target surface during the process of freezing. This lateral transfer process, which is treated analytically in appendix A, results in an additional, positive, contribution to S of the form $K_3F_3\tau_fL(\rho_o - \rho_I)$, where K_3 is a constant which depends upon factors such as the droplet size distribution, the shapes of the frozen droplets and the topography of the target surface; F_3 is a ventilation coefficient, τ_f is the freezing time of a droplet on the target surface and ρ_o is the saturation vapour density of water at 0 °C. The physical model to which this term refers is the lateral transfer of vapour, at a rate proportional to $(\rho_o - \rho_I)$, from freezing droplets whose number at any given time is roughly proportional to τ_fL. Thus

$$S = K_3F_3\tau_fL(\rho_o - \rho_I) + K_1F_1(\rho_W - \rho_I)/R - K_2F_2(\rho_W - \rho_I)/d. \quad (1)$$

As the parameters in this equation vary with temperature and time during an experiment, it is in principle possible that S can take on both positive and negative values. In the succeeding discussion we assume this to be the case. We also assume that variations in K_1, K_2, K_3 are much smaller than those in τ_f, L, ρ_W and ρ_I, and can thus be neglected. We also assume the ventilation terms F_1, F_3 and F_2 ($\sim$1) are constant.

Calculations of the freezing time τ_f are presented in appendix A. The product $\tau_f(\rho_o - \rho_I)$ can thus readily be determined, and (together with τ_f) is shown in Fig. 6 to decrease steadily as the temperature T falls. Thus, from Eq. (1), our hypothesis predicts that positive charging of the target is most likely to occur at the highest temperatures, and negative at the lowest. This accounts for point (3) in the summary at the end of section 2.

Point (4), which is concerned with the influence of liquid water content on the sign of the charging, is also explicable in terms of our hypothesis. We see from Eq. (1) that S becomes more positive as L increases, and thus the target grows faster by means of lateral diffusion. Therefore, the reversal temperature is lower with increased L. Points (1) and (2) constitute the basis of our hypothesis, which is therefore consistent with all four points listed in section 2.

We now enquire whether an examination of Eq. (1) yields an explanation for the current/time curves presented in Fig. 1. We examine initially the major features of these curves, and disregard the initial positive peak and the time delay between the minima in L and I: these points are discussed later. It is necessary to note at this point that, according to our hypothesis, S governs only the *sign* of the charging. The magnitude depends sensitively upon the size of the colliding ice crystals, their concentration and the event probability, all of which, as shown by Jayaratne *et al.* (and in Fig. 3), change substantially throughout the course of an experiment. Jayaratne *et al.* found that $I \propto d^a$ where a ranged from about 3·5 to 5.

At the highest temperatures $\tau_f(\rho_o - \rho_I)$ is a maximum, and therefore positive charging will occur throughout the duration of a run, as observed (Figs. 1(a), 1(b)). At intermediate temperatures the current will be initially positive, since L is a maximum, fall to negative values as L drops towards its minimum value, and rise again to positive values as L is regenerated owing to ice crystal fall-out (Fig. 1(c)). As the temperature drops further the reduction in $\tau_f(\rho_o - \rho_I)$, coupled with the fact that L is always lower at the end of an experiment than at the beginning, will cause S to tend to be negative throughout a run (Fig. 1(d)). However, at the very lowest temperatures employed, the term $(\rho_W - \rho_I)$ becomes so small that the first term in Eq. (1) plays a more substantial role, causing positive charging to occur as L increases towards the end of a run

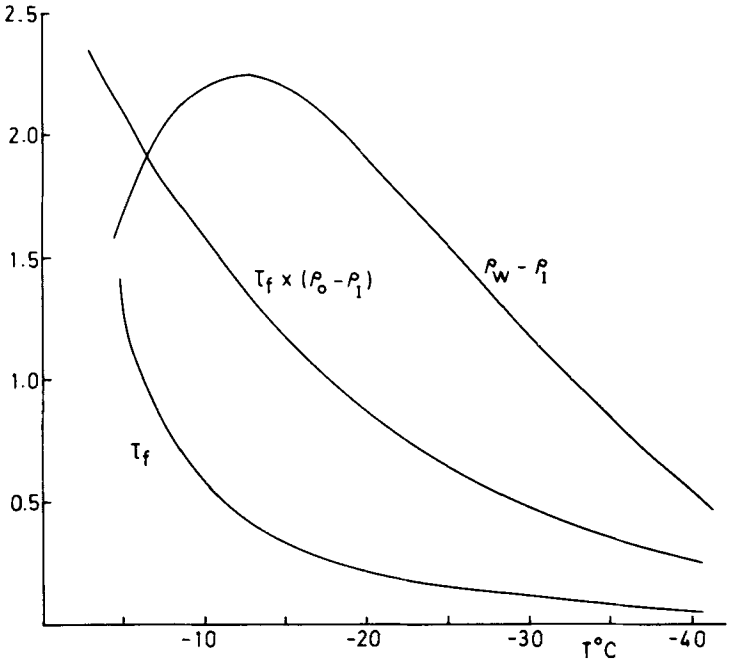

Figure 6. The calculated variation with temperature of $[\rho_w - \rho_I]\,(g\,m^{-3}\times 10)$, τ_f(ms), and $[\tau_f(\rho_o - \rho_I)]$ (arbitrary units).

(Fig. 1(e)). Thus the time dependence of all five curves in Fig. 1 is seen to be qualitatively consistent with our hypothesis.

The two features of the curves in Fig. 1 which remain to be explained are the 'initial positive peak' and the 'time delay' of about one minute between the minima in L and maxima in (negative) I. These are both attributable, in our view, to properties of the laboratory cloud which are not considered in formulating Eq. (1). The concentration of ice crystals in the cloud is very high ($\sim 1000\,cm^{-3}$) at the beginning of a run, and the cloud is not well mixed since the ice crystals are nucleated in concentrated filaments or clumps and do not readily disperse. Thus a large fraction of the initial crystals will have crystals rather than droplets as nearest neighbours and will therefore not be growing at water saturation. Consequently, we attribute the initial positive peak to the fact that the cloud is unmixed, most of the crystals are growing from the vapour more *slowly* than the target and thus I is positive. Also, L is a maximum at the beginning of a run. As time passes the crystals grow and thus (positive) I increases. Eventually, however, the cloud becomes more homogeneous, more crystals grow faster than the target and the initial positive charging diminishes. Further evidence on this question is presented in the following section.

The time delay effect can be explained in a similar manner. When L reaches its minimum value, S and therefore I are negative, as discussed earlier. However, a substantial fraction of the crystals in this water-depleted environment will not be growing swiftly, and thus the negative charging of the target will be relatively small. As the droplet population is regenerated, a greater proportion of crystals grow effectively and thus I increases (negatively). As L continues to increase, however, the riming (lateral transfer) term becomes more important and I passes through a (negative) maximum and thereafter diminishes. As L increases further, I may reverse to become positive. This pattern is consistent with that displayed in Fig. 4.

We conclude that our rudimentary hypothesis, based on the relative diffusional growth rates of the colliding hydrometeors, is able to explain, in a qualitative sense, all the results presented in section 2.

4. Further laboratory experiments

In this section we describe some additional experiments designed to test further our charging hypothesis and to learn more about the associated mechanism of charge transfer.

Experiments designed to explore the growth rate/charging relationship were performed using a stationary target (a simulated soft hailstone), as described by Jayaratne *et al.* The target was an ice-coated brass rod of diameter 5 mm and length 10 mm mounted vertically in a horizontal brass tube of internal diameter 25 mm. Ice crystals were drawn past the target at a constant speed. The target could be heated or cooled relative to the environmental temperature—maintained generally at −10 °C—by means of a thermoelectric element. Thus its growth rate relative to the ice crystals could be reduced or increased. A thermocouple attached to the target by means of a dab of heatsink compound provided a rough measurement of its surface temperature. Any current flowing to the target was amplified and detected by means of a sensitive electrometer.

A supercooled droplet cloud was seeded to produce ice crystals, which quickly exhausted the liquid water in the cloud. Current was passed through the thermoelectric element in order to change the target temperature, and crystals alone were then drawn past at a constant speed of 15 m s^{-1}. (Low flow speeds could not be employed because the charging current I was then undetectable.) The target achieved temperature equilibrium in the flow in about 20 s, at which point I was noted. The concentration and mean size of the ice crystals were about 600 cm^{-3} and 25 μm respectively. I was negative when the target was at the same temperature as the crystal cloud, or when it was warmer, but cooling it marginally (by less than 1 degC) caused I to become positive. This current/temperature difference (ΔT) behaviour and the sharpness of the sign transition are illustrated in Fig. 7. For both positive and negative charging, I remained almost constant as ΔT was raised above the small value required to effect the sign reversal. The glaciated cloud must have been close to ice saturation, and the ice crystals contained within it grew

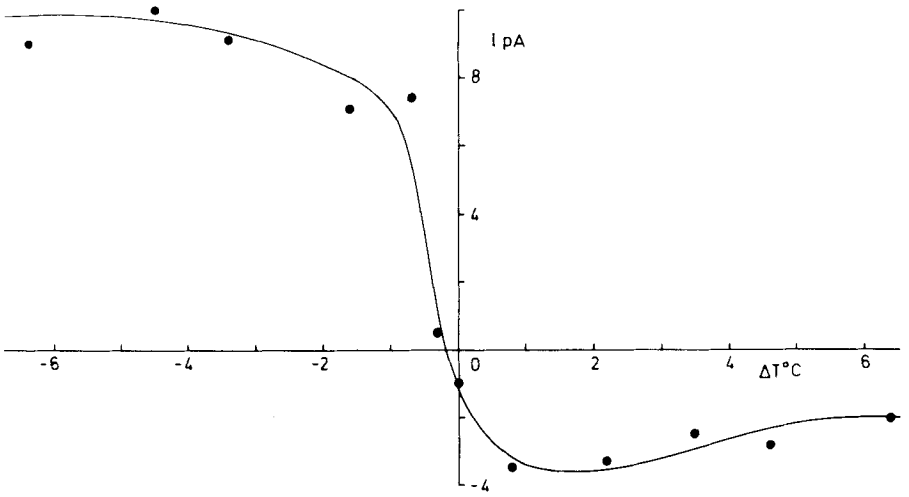

Figure 7. The charging current I to the stationary target as a function of the temperature difference ΔT between the target surface and a cloud consisting entirely of ice crystals. $U = 15$ m s^{-1}. $T \simeq -10$ °C. Experimental error: I ±20%; ΔT ±0·25 degC.

or evaporated only very slowly. Cooling the target would have increased its growth rate from the vapour, but the insensitivity of I to ΔT suggests that the *magnitude* of the charge transfer—as distinct from the sign—is not a sensitive function of the relative growth rates of the interacting hydrometeors. We see that the $I/\Delta T$ patterns are qualitatively consistent with the hypothesis advanced in section 3. The estimated values of I in these experiments are about three orders of magnitude less than the maximum values obtained, for otherwise identical conditions, when water saturation exists within the mixed-phase cloud. This result is consistent with that obtained by Jayaratne *et al.*

This absence of a significant dependence of the *magnitude* of I upon the temperature difference (and therefore relative growth rates) was further examined by sucking crystal-laden air past a stationary target which had been dipped into liquid nitrogen and was warming up towards ambient temperature. I was essentially independent of ΔT: the positive current to the target remained roughly constant as ΔT decreased from 20 degC to a few degrees.

The above experiments demonstrate again that both hydrometeors must be growing for significant charge transfer to occur. In order to test directly our hypothesis, which deals with the more significant charge transfer of the primary experiment—and is more representative of the thunderstorm environment—the same heating/cooling experiment was repeated at water saturation at $-10\,^{\circ}$C. A cloud of very small droplets was produced using the technique of Mossop, mentioned earlier, and thus water saturation existed in conditions when riming was insignificant. (It had been established, in a separate experiment, that if riming was allowed to occur, its effects masked those due to imposed temperature differences.) The stationary target was exposed to the crystal flow immediately after the current record from the moving target experiment, running simultaneously, indicated that I was negative, following the initial positive excursion, and L was close to its minimum value. With no heating or cooling of the stationary target the current flowing to it was also negative. Despite considerable scatter in the results—probably due to fluctuations in the vestigial riming rate—it was clear that if the target was warmed relative to the mixed-phase cloud, I remained negative but that cooling it by at least 1 degC below the ambient temperature caused the current to reverse sign to positive. Thus the current/ΔT (relative growth rate) pattern is identical to that obtained in the experiments conducted at ice saturation, and is therefore explicable in terms of our relative growth rate hypothesis. The magnitude of I in these experiments was about 20 times greater than that measured in the ice saturation studies: note that I was relatively small in these experiments since they were performed when L was close to its minimum value.

Further support for the hypothesis is provided by the small-droplet cloud (insignificant riming) studies performed with the stationary target in conditions where I was positive in the absence of imposed temperature differences. Heating the target by a modest amount (less than 1 degC), using the thermoelectric element, was found to reverse the sign of charging to negative.

An experiment was performed with the rotating target apparatus in order to test the argument, presented in section 3, that the initial positive peak in the current/time curves (Fig. 1) was due to inhomogeneities in the ice crystal distribution within the cloud, which caused the average crystal growth rate to be reduced. The supercooled cloud, consisting of droplets large enough to engage in riming, was glaciated in the normal manner, and as the run proceeded the rod was stopped for a short time, thus preventing mixing of the continuously arriving droplets, then restarted. The current/time curves obtained in a typical experiment are illustrated in Fig. 8. It is seen that although I was negative just before the rotation was stopped, a sharp positive peak occurred immediately after the rotation recommenced, followed by the negative charging characteristic of the tem-

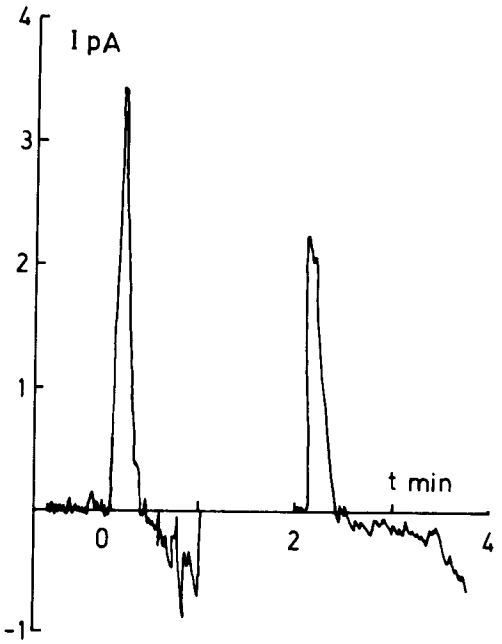

Figure 8. The charging current I to the moving target as a function of time t. $T \approx -24°C$. $U = 3\,m\,s^{-1}$. The cloud was seeded at $t = 0$. Rotation was stopped at $t = 1$ min and re-started at $t = 2$min.

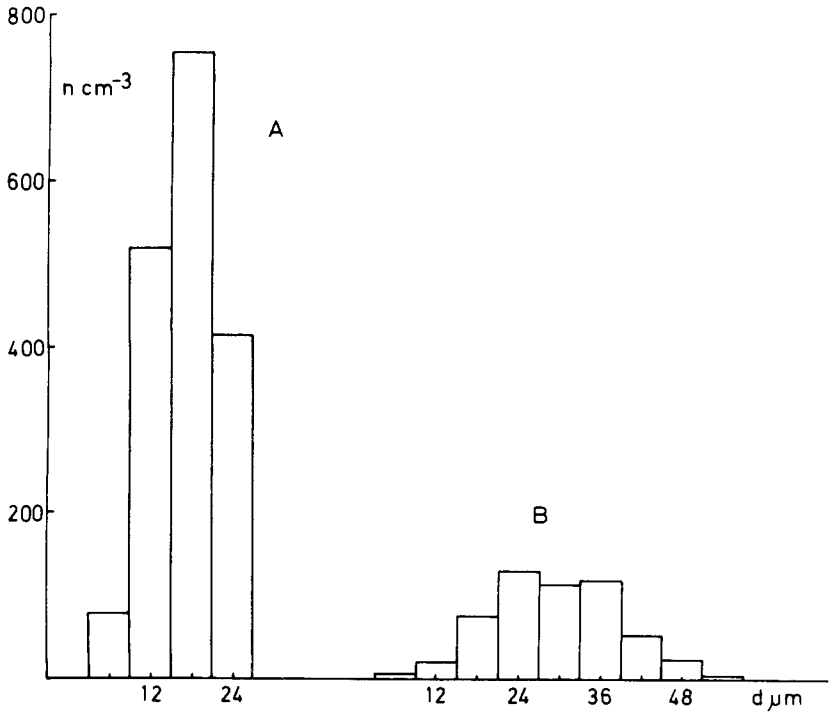

Figure 9. Ice crystal size distributions $n(d)$ one minute after seeding. A, well mixed cloud; B, unmixed cloud. $T = -26°C$.

perature (−24 °C) employed. A series of such positive peaks could be obtained by stopping and restarting the rod, provided there were crystals in the cloud. These observations support our earlier conclusion that the ice crystal cloud is initially highly inhomogeneous within the chamber, but becomes more uniform because of the stirring induced by the rotating apparatus. When the rotation ceases, the higher localized influx of water vapour into the chamber recreates inhomogeneity. Further evidence in favour of these ideas is provided by Fig. 9, which presents histograms of ice crystal size measured in the cloud one minute after seeding, (A) when movement of the target was continuous throughout this period, and (B) when it was held stationary; whereupon the unmixed cloud leads to a range of crystal growth rates and sizes.

In order to test the explanation given in section 3 for the observed time delay of about one minute between the achievement of minimum L and maximum (negative) I, a special experiment was conducted at −22 °C with the rotating target apparatus and a supercooled droplet cloud with the standard size distribution. Just before I reached its peak negative value the droplet supply rate was reduced whereupon, as shown in Fig. 10, the negative charging diminished. About one minute later the supply rate was increased to its original value, whereupon I increased negatively and then became positive. The negative charging here may be attributed to the high crystal growth rate. The reduction in droplet supply diminished the number of growing crystals and hence reduced the target charging rate. With the re-established droplet supply, more crystals were able to grow efficiently and the hailstone charging rate increased. Eventually, the crystal concentration diminished and hence L increased, which permitted the target to charge positively due to increased diffusional growth rate via lateral transfer.

We conclude that the experiments described in this section provide additional support for the hypothesis and arguments advanced in section 3.

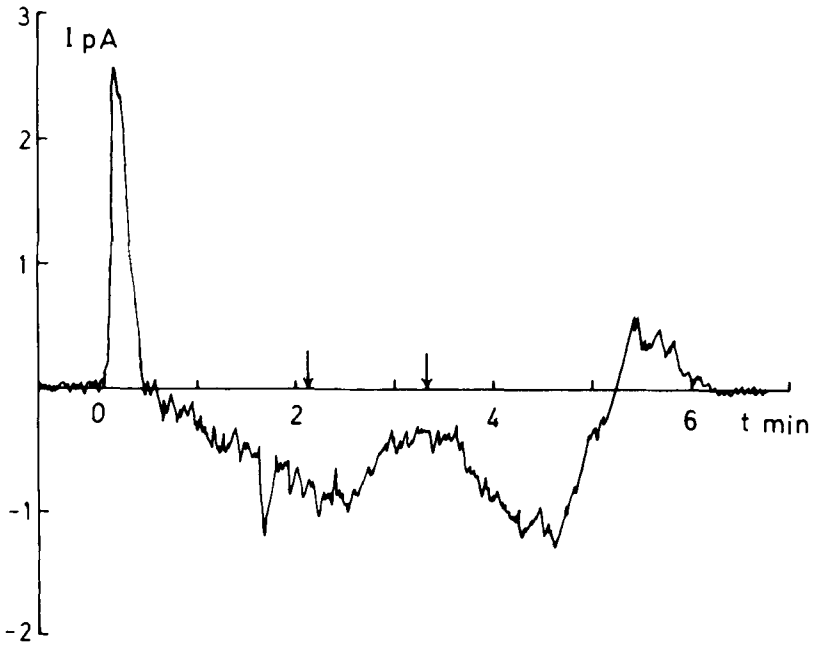

Figure 10. The charging current I to the target as a function of time t. $T = -22$ °C. $U = 3\,\mathrm{m\,s^{-1}}$. The vapour supply was reduced at 2 min 10 s, and re-established at 3 min 15 s, as indicated by the arrows.

5. Discussion and application to charging in thunderstorms

The results of the experiments described in sections 2 and 4 are all explicable qualitatively in terms of the simple hypothesis discussed and developed in section 3; namely that appreciable charging requires both the ice crystals and the target with which they collide to be growing from the vapour, and that the *sign* of the charging is determined by some (unknown) property associated with the relative diffusional growth rates of the interacting hydrometeors, the faster growing surface becoming positively charged.

This hypothesis is non-quantitative. Equation (1) does not take account of factors such as the observed inhomogeneity in the ice crystal cloud, variations in growth rates over the different faces of the ice crystals, droplet spreading on impact, the surface topography of the target, the 'twin-band' nature of the rime deposits (Fig. 5), which restricts the area of accretion, etc., and we conclude that at this stage we are unable to quantify our treatment with an adequate degree of confidence. Nor have we proved quantitatively in our experiments that the charging of the target changes from negative to positive at the point at which it starts to grow from the vapour faster than the crystals. We have simply shown that increasing the diffusional growth rate of the target relative to that of the crystals can cause this sign reversal; and correspondingly, that decreasing the growth rate relative to the crystals can cause the target charging to change from positive to negative. The diffusional growth rate of a riming soft hailstone will be highly non-uniform over its surface, with maximum growth rates in the immediate vicinity of the freezing droplets (appendix, Eq. (22)).

The mechanism responsible for significant charging in these experiments is unknown, though it is clearly related in some way to the surface properties of the interacting hydrometeors while they are growing from the vapour. It is probably premature to speculate on its nature on the basis of the evidence available. Contact potential differences between ice surfaces formed in different ways, which have been studied extensively by Caranti and Illingworth (1980), do not appear, by themselves, to offer an explanation for our observations. They find that the contact potentials are identical for growing and evaporating unrimed surfaces, and are independent of the rates of growth or evaporation. However, our experiments reveal that: (1) collisions involving ice crystals which are growing effectively produce charging currents several orders of magnitude greater than in the case of crystals that are not; and (2) the sign of the charging can be reversed by changing the relative growth rates of the interacting hydrometeors.

Illingworth (1985) has advanced the hypothesis that negative charging of an ice surface is a consequence of contact potential differences between the surface and that of the colliding crystals. This effect is opposed to, and can be overcome at higher temperatures by, positive charging associated with collisions of the crystals with localized regions of the surface where the freezing of supercooled droplets has produced additional vapour deposition. The physics of this latter process are not defined, and the sign reversals which can be created in our stationary target experiments by the application of temperature (and thus relative growth rate) differences in the absence of riming do not appear to be consistent with this idea.

In an attempt to assess the applicability of the research described in the foregoing sections to the problem of thundercloud electrification, we make use of the one-dimensional model of Illingworth and Latham (1977). Soft hailstones of radius R and density σ_i grow by accretion of supercooled water as they fall with a velocity V against an updraught U which carries ice crystals, of concentration n_x and size d, through a cylindrical region (the charging zone) of depth Z_m and upper and lower temperature, T_o and T_m respectively, the lapse rate being constant between these levels. For the sake of simplicity,

it is assumed that each collision between a soft hailstone and an ice crystal within this zone results in the separation of charge

$$q = A_1 d^a V^b \tag{2}$$

where A_1, a and b are constants. n_x, U, σ_i and the liquid water content L are constant throughout the charging zone, at the top of which soft hailstones have a fall velocity $V_o = U$. V is related to R by

$$V = A_2 R \tag{3}$$

where A_2 is a constant (Chisnell and Latham 1976). Thus at the top of the charging zone the soft hailstones have a radius

$$R_o = U/A_2 \tag{4}$$

while at the bottom they have a radius R_m. The concentration of soft hailstones at a level where their velocity is V is

$$N = A_3/(V - U) \tag{5}$$

where A_3 is a constant. The dynamical and microphysical properties of the cloud at any level are assumed to be independent of time. Further details of the model are provided by Illingworth and Latham.

The mixed-phase cloud is at water saturation, so the crystals and the soft hailstones are growing from the vapour. Thus the conditions within the charging zone are similar to those existing in the primary experiments described herein, and also those regions of a thundercloud in which Dye *et al.* (1986) found significant electric fields. In the Montana thundercloud studied by these workers, the charging region was subadiabatic, and the crystals were probably introduced into it via turbulent exchange with an adjacent downward-moving glaciated region, i.e. the crystals were probably initiated at cloud top.

The charging rate per unit volume of cloud, resulting from rebounding collisions between soft hailstones and ice crystals, is given by

$$dQ/dt = NR^2 V n_x q \tag{6}$$

which, using Eqs. (2), (3), (4) and (5), can be rewritten as

$$\frac{dQ}{dt} = \frac{A_4 n_x d^a R^{2+b}}{(1 - R_o/R)} \tag{7}$$

where A_4 is a constant. If we assume, on the basis of the experiments of Jayaratne *et al.*, and those described herein, that $a \sim 4$ and $b \sim 2$ we have

$$\frac{dQ}{dt} = \frac{A_4 n_x d^4 R^4}{(1 - R_o/R)}. \tag{8}$$

Equation (8) was solved, using the expression for soft hailstone growth rate given by Illingworth and Latham, in order to determine the relationships between dQ/dt and Z (or T). In the majority of calculations performed it was assumed that $T_o = -20\,°C$, $T_m = -6{\cdot}4\,°C$, $Z_m = 3{\cdot}2\,km$, $L = 1{\cdot}0\,g\,m^{-3}$, $\sigma_i = 0{\cdot}5\,g\,cm^{-3}$, $U = 2{\cdot}0\,m\,s^{-1}$ and $A_2 = 4000\,s^{-1}$, these values being based on the observations of Dye *et al.* and the work of Illingworth and Latham. In these circumstances, $R_o = 0{\cdot}5\,mm$ and $R_m = 3{\cdot}0\,mm$. The rate of growth of the ice crystals was calculated using a simplified form of the standard expressions given by Pruppacher and Klett (1978). Three separate formulations were used for the estimated variations with altitude of the ice crystal concentration n_x: (1) is based on the glaciation mechanism described by Hallett and Mossop (1974) in which

crystals are produced by riming in a narrow temperature band around −7 °C which corresponds to the bottom of the charging zone. In this case, we assume

$$n_x/n_o = 1 \tag{9}$$

throughout the zone, where the normalizing constant n_o is the concentration of crystals at its base. (2) is based on activation on ice nuclei, whose concentration increases with decreasing temperature T in the manner reported by Fletcher (1962), i.e.

$$n_x/n_o = \exp[0{\cdot}6(T_m - T)]. \tag{10}$$

(3) attempts, in a rudimentary way, to simulate glaciation by means of lateral turbulent transfer of ice crystals into the charging zone from an adjacent penetrative downdraught. If we assume that the rate of transfer is independent of altitude then it is readily shown that

$$n_x/n_o = 1 - \exp(-\alpha z') \tag{11}$$

where in this case the normalization constant n_o is the concentration of ice crystals in the adjacent downdraught and α (generally assumed to possess a value of 1 km^{-1}) is a mixing parameter: z' is the height above the base of the charging zone where $T = T_m$. Equation (11) predicts that the ice crystal concentration in upward-moving, sub-adiabatic supercooled regions of convective clouds increases slowly with altitude. Its normalized values fit reasonably well with those measured by Choularton and Heapy (private communication) in clouds studied in the CCOPE experiment in 1981, in which the dominant mechanism of glaciation was nucleation at cloud top, followed by vertical transport in penetrative downdraughts.

Approximate solutions to Eq. (8) are presented in Table 1 for the three mechanisms of glaciation. Note that the charging rates in each of the three cases have been normalized

TABLE 1. CHARGING RATES (IN ARBITRARY UNITS) FOR THE THREE GLACIATION MECHANISMS, AS A FUNCTION OF TEMPERATURE T AND DISTANCE Z, MEASURED DOWNWARDS FROM THE TOP OF THE CHARGING ZONE

		Charging rate		
T (°C)	Z (km)	1	2	3
−8	3·0	1·0	1·0	1·0
−9	2·9	2·5	1·4	1·5
−10	2·7	4·2	1·9	1·9
−11	2·6	6·1	2·5	2·1
−12	2·4	8·2	3·4	2·4
−13	2·3	9·8	4·4	2·5
−14	2·1	11·6	6·0	2·6
−15	2·0	12·5	7·9	2·5
−16	1·8	13·1	10·2	2·4
−17	1·7	13·8	13·7	2·3
−18	1·6	13·6	17·4	2·1
−19	1·4	13·0	22·1	1·9
−20	1·3	12·2	27·7	1·7
−21	1·1	11·1	34·5	1·5
−22	1·0	9·9	42·4	1·3
−23	0·8	8·7	51·6	1·1
−24	0·7	7·0	58·2	0·8
−25	0·6	5·5	64·3	0·6
−26	0·4	4·2	69·4	0·5
−27	0·3	3·1	73·5	0·3
−28	0·1	1·9	66·2	0·2

to that calculated at $T = -8\,°C$. The constant A_4 takes on a different value for each of the glaciation mechanisms, so comparisons between them cannot be made. The objective of these rudimentary calculations is simply to examine, for each mechanism separately, the relationship between charging rate and temperature (or altitude).

Table 1 shows that in the case of mechanism (1), the charging is most effective between about $-15\,°C$ and $-20\,°C$. For mechanism (2) the charging rate is dominated by the high sensitivity of n_x to T (Eq. (10)), and this increases rapidly with altitude. The charging rate for mechanism (3) varies much more slowly with temperature, but peaks around $-14\,°C$ for the case described. If the downdraught supplying the ice crystals penetrates only to the $-12\,°C$ level (instead of to the bottom of the charging zone) the charging rate peaks at about $-22\,°C$, while if it penetrates only to the $-20\,°C$ level the charging rate is a maximum around $-26\,°C$. The conclusions from these crude calculations are—for all three mechanisms—quite insensitive to reasonable variations in the governing parameters.

The work described herein, coupled with various earlier laboratory experiments (e.g. Takahashi 1978; Gaskell and Illingworth 1980; Jayaratne *et al.* 1983), in which soft hailstone/ice crystal collisions have been simulated, have yielded sign reversal temperatures varying from $-10\,°C$ to $-20\,°C$, which suggest, in the light of the foregoing calculations, that soft hailstones will generally acquire negative charge when they make rebounding collisions with ice crystals. This argument is only circumstantial, however. In fact, the insensitivity of charging rate to temperature predicted for mechanism (3) and (especially) mechanism (1) suggests that under some circumstances the parameter values may be such that reverse polarity (negative above positive) thunderclouds may occur, which is consistent with the observed large fraction of lightning strokes which bring positive charge to earth in wintertime storms over the eastern seaboard of the U.S.A. (Orville 1987) and over Alabama (Christian, private communication). Before this argument can be developed further the link between the laboratory studies and the natural situation must be better understood, and a field growth model established which takes full account of the interrelated dynamical, microphysical and electrical processes occurring within thunderclouds.

Acknowledgments

We are grateful for the support provided by the National Science Foundation (Grant ATM 842016), the Natural Environment Research Council (Grant GR3/4947A) and the University of Washington Visitor Programme.

Appendix A

Lateral flux and freezing time calculations

In this section we describe three separate studies which provide information employed elsewhere in this paper. Calculations are presented of the lateral flux of vapour from a droplet to the soft hailstone upon which it is freezing; this relates to the first term in the expression for S in Eq. (1). We also present a new calculation of the droplet freezing time τ_f, which is present in the same term. A brief account is presented of experiments designed to provide values of ventilation coefficients.

The situation envisaged in the lateral flux calculation is considerably simplified from reality, and is illustrated in Fig. A.1(a). A supercooled droplet of original radius a' is freezing as a hemisphere of radius a ($=2^{1/3}a'$) on a spherical ice surface of radius R. The droplet surface remains at $0\,°C$ for the period τ_f during which it is freezing. The ice

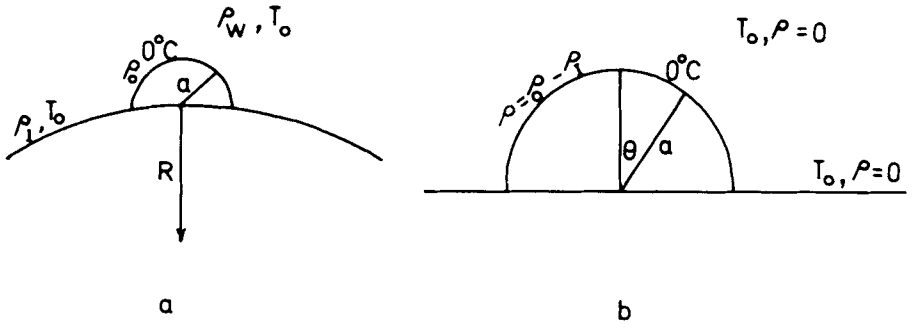

Figure A.1. A hemispherical water droplet freezing onto the surface of a soft hailstone of radius R. ρ_W and ρ_I are the saturation vapour densities with respect to water and ice respectively, at the ambient air temperature T_o. ρ_o is the saturation vapour density at 0°C. (a) The actual situation envisaged. (b) Scheme employed in the calculations, as described in the text. ρ is the vapour density.

surface and the ambient air are assumed to be everywhere at a temperature T_o. Since $a/R \ll 1$ the ice surface may be regarded as a flat plane from the viewpoint of the droplet freezing on its surface. The surrounding air is assumed to be at water saturation. The vapour densities at the surface of the freezing droplet, at the surface of the soft hailstone and in the surrounding air are respectively the saturation density with respect to water at 0 °C, ρ_o, the saturation vapour density with respect to ice at T_o, ρ_I, and the saturation vapour density with respect to water at T_o, ρ_W. We assume the vapour fields remain constant over the freezing time of a drop, and the vapour diffusion takes place in steady state.

Since Laplace's equation $\nabla^2\rho = 0$, where ρ is the vapour density, is linear and homogeneous we can subdivide our calculation of the vapour flux to the soft hailstone into two parts—both of which can readily be treated—and sum the solutions. The first disregards the freezing drop and concerns simply a spherical ice surface at temperature T_o in air at T_o. The second is illustrated in Fig. A.1(b). The hemispherical droplet has a vapour density at its surface of $\rho = \rho_o - \rho_I$, while freezing on a soft hailstone with zero vapour density at its surface, this process occurring in an environment with zero vapour density.

For the first situation, the far-field vapour flux to the soft hailstone surface, ψ_1, is given by

$$\psi_1 = -D\nabla\rho|_{r=R} = D(\rho_W - \rho_I)/R \tag{12}$$

where D is the diffusion coefficient for water vapour in air. Or, since the soft hailstone is ventilated,

$$\psi_1 = fD(\rho_W - \rho_I)/R \tag{13}$$

where f is the ventilation coefficient. This is the far-field contribution to the soft hailstone growth; the second term in Eq. (1).

In the absence of ventilation and assuming a steady-state situation, the solution to the second component is

$$\rho = \sum_{l=0}^{\infty} [A_l r^l + B_l r^{-(l+1)}] P_l(\cos\theta) \tag{14}$$

where $P_l(x)$ are Legendre polynomials, r is the radial distance and θ is the angle illustrated in Fig. A.1.

From the boundary condition $\rho = 0$ at $r = \infty$ we see that $A_l = 0$ for all l. From the boundary condition $\rho = 0$ at $\theta = 90°$ we see that $B_l = 0$ for even values of l. Thus Eq. (14) reduces to

$$\rho = \sum_{n=0}^{\infty} \frac{B_{2n+1}}{r^{2n+2}} P_{2n+1}(\cos\theta). \tag{15}$$

From the boundary condition $\rho = \rho_0 - \rho_I$ at $r = a$ (at the surface of the freezing droplet) we obtain

$$\rho_0 - \rho_I = \sum_{n=0}^{\infty} \frac{B_{2n+1}}{a^{2n+2}} P_{2n+1}(\cos\theta) \tag{16}$$

which, together with the orthogonality of the P_l gives

$$B_{2n+1} = (4n+3)a^{2n+2}(\rho_0 - \rho_I)\int_0^1 P_{2n+1}(x)\,dx. \tag{17}$$

Thus

$$B_1 = 3(\rho_0 - \rho_I)a^2/2 \tag{18}$$

$$B_3 = -7(\rho_0 - \rho_I)a^4/8 \tag{19}$$

etc. Therefore, from (15), (18) and (19),

$$\rho = \frac{3(\rho_0 - \rho_I)a^2\cos\theta}{2r^2} - \frac{7(\rho_0 - \rho_I)a^4(5\cos^3\theta - 3\cos\theta)}{16r^4} + \ldots. \tag{20}$$

The vapour flux to the hailstone surface ($\theta = 90°$) from a single drop is given by

$$\psi_2 = -D\nabla\rho|_{\theta=90°} = D(\rho_0 - \rho_I)\left[\frac{3a^2}{2r^3} + \frac{21a^4}{16r^5} + \ldots\right]. \tag{21}$$

This series converges for all $r > a$, but diverges at $r = a$ because the boundary condition assumes a discontinuity at $r = a$, $\theta = 90°$, which is not physically realistic. Thus the solution (21) is not valid very close to the droplet, but elsewhere is acceptable and dominated by the first term. Accordingly, to a reasonable approximation, and assuming a ventilation factor f_3, we obtain

$$\psi_2 = \frac{3f_3 D(\rho_0 - \rho_I)a^2}{2r^3}. \tag{22}$$

This is the lateral diffusion contribution to the soft hailstone growth, made by a single droplet.

If we assume that the ventilation factors for the soft hailstone and the freezing droplet are identical ($f_1 = f_3$), we see from Eqs. (13) and (22) that the radial distance r^* at which the lateral diffusion and deep-field contributions to soft hailstone growth from the vapour are equal is given by

$$r^* = \left(\frac{3a^2R(\rho_0 - \rho_I)}{2(\rho_W - \rho_I)}\right)^{1/3}. \tag{23}$$

In a typical laboratory experiment at $-20\,°C$, $a \sim 9\,\mu m$, $R \sim 2{\cdot}5\,mm$, $(\rho_0 - \rho_I) \sim 4\,g\,m^{-3}$, $(\rho_W - \rho_I) \sim 0{\cdot}19\,g\,m^{-3}$, which yields $r^* \sim 180\,\mu m$. Thus the contribution of lateral vapour flux from freezing droplets to the depositional growth of the soft hailstone is likely to be

significant over some non-trivial fraction of surface. The localized regions where this effect is appreciable will not be circularly symmetric round each freezing droplet because of distortion of the vapour flow by ventilation.

The mass of vapour flowing per unit time from the surface of a freezing droplet (dM/dt) may be determined by integrating Eq. (21) over the soft hailstone surface, or by finding ψ at $r = a$ from Eq. (20) and integrating over the droplet surface. In either case, we obtain—when we disregard all terms in the series except the first, and incorporate ventilation,

$$dM/dt = 3\pi f_3 Da(\rho_o - \rho_I). \tag{24}$$

Thus the total mass lost by vapour transfer during the freezing of a droplet is approximately

$$\Delta M = 3\pi f_3 Da(\rho_o - \rho_I)\tau_f. \tag{25}$$

The characteristic time for vapour diffusion from the freezing droplet

$$\tau_d \sim a^2/D \tag{26}$$

is about 5 μs for the conditions of our experiments. This is much less than the freezing time τ_f, and thus our assumption of steady state is justified.

The characteristic time for ventilation to remove vapour from the hailstone is

$$\tau_v \sim R/U \tag{27}$$

where U is the ventilation speed. For the conditions of our experiments $\tau_v \sim 1$ ms, which is much larger than τ_d, and thus it is legitimate to assume that the vapour emanating from the freezing droplets will be deposited upon the hailstone.

In calculating the freezing time τ_f for a droplet it is necessary to take account of heat loss both to the air and to the ice substrate. We first calculate separate expressions for τ_f, for each mechanism of heat loss acting alone.

The solution in the case of heat loss to the substrate only is applicable to many drop shapes ranging from approximately hemispherical to thin films if the surface of the substrate is flat, and to the latter case (large spreading) if the surface is irregular on the scale of the freezing event—as may often be the case in nature.

In addition to the conventional assumption that the first stage of the freezing process (during which the temperature of the droplet rises to 0°C) occupies only a small fraction of the total freezing time, during the remainder of which $T = 0$°C, we make two additional assumptions. The first is that the freezing front is always parallel to the plane of the interface, i.e. the heat flow is always perpendicular to the substrate surface. The error associated with ignoring edge effects will be less in situations where the drop spreads substantially before freezing, since the ratio of interfacial area to edge length will be greater. It will also be less if the width of the substrate is limited (i.e. if the droplet is freezing onto a column or an already frozen droplet, rather than a flat surface of dimension large compared with the droplet size), because lateral heat flow is again constrained.

This perpendicular heat flow assumption makes the treatment of our problem versatile, since the shape of the drop enters only through its height a, which is also the distance the freezing front must travel. Thus, for example, the freezing time for a hemispherical cap of height a is the same as that of a uniform layer of identical thickness on an infinite half-plane.

If at time $t = 0$ the surface of an infinite half-plane of temperature T_o is suddenly

raised to 0°C the flux of heat into the surface (Carslaw and Jaeger 1959) is

$$\psi = K_I T_o/(\pi k_I t)^{1/2} \tag{28}$$

where K_I and k_I are the thermal conductivity and thermal diffusivity of ice, respectively. These parameters are related by means of

$$k_I = K_I/C_I\sigma_I \tag{29}$$

where C_I and σ_I are the specific heat and density of ice respectively.

The second particular assumption is that this solution applies to the freezing front. Since the front is moving away from the substrate the temperature gradient across it and therefore the heat flow through it will be less than given by Eq. (18) (this error is discussed later).

The total heat per unit area which has been conducted through the freezing front after a time τ_{fs} will be (from Eq. (18))

$$\int_0^{\tau_{fs}} [K_I T_o/(\pi k_I t)^{1/2}]\, dt \tag{30}$$

and this must equal the latent heat released per unit area by the freezing droplet, which is

$$b\sigma_W(L_f - C_W T_o), \tag{31}$$

where σ_W is the density of water, L_f is the latent heat of freezing and C_W the specific heat of water. Note that $(L_f - C_W T_o)/L_f$ is the fraction of the droplet remaining in liquid form after the first stage of freezing. Thus from Eqs. (29), (30) and (31) we obtain

$$\tau_{fs} = \frac{\pi b^2 \sigma_W^2 (L_f - C_W T_o)^2}{C_I 4\sigma_I K_I T_o^2}. \tag{32}$$

The error in the first particular assumption will lead to an overestimate of τ_{fs}, and that in the second will lead to an underestimate.

Macklin and Payne (1967) performed a very similar calculation, for a hemispherical droplet only. With the same first assumption and the same expression for ψ, but assuming that the freezing front is stationary (i.e. not taking account of its decreasing area as freezing proceeds) they underestimated τ_{fs} by an additional factor of 4/9.

Our calculation of the freezing time τ_{fa}, when all the heat loss is to the surrounding air, via conduction and evaporation, is performed for a hemispherical droplet only. The rate of loss of heat from the (ventilated) droplet by means of evaporation is given (Eq. (24)) by

$$L_v\, dM/dt = 3\pi L_v f_3 Da(\rho_o - \rho_I) \tag{33}$$

where L_v is the latent heat of vaporization of water. The analogous rate of heat loss by conduction is

$$3\pi K_a T_o f_3 a \tag{34}$$

where K_a is the thermal conductivity of air. The latent heat released by the droplet on freezing is

$$2\pi a^3 \sigma_W (L_f - C_W T_o)/3 \tag{35}$$

where σ_W is the density of water. Thus from (33), (34) and (35) we obtain

$$\tau_{fa} = \frac{2\sigma_W a^2 (L_f - C_W T_o)}{9 f_3 [L_v D(\rho_o - \rho_I) + K_a T_0]}. \tag{36}$$

A treatment of a similar problem by Macklin and Payne provided an expression for τ_{fa} which is greater than that in Eq. (36) by a factor of approximately $1{\cdot}5f_3$. This is because they took no account of the proximity of the soft hailstone, which acts as a sink for the vapour and heat emitted by the freezing droplet or ventilation effects.

Values of the overall freezing time τ_f, which takes account of heat loss both to the substrate and to the air, were determined as follows, and are plotted in Fig. 6. τ_{fa} was calculated from Eq. (36), together with the magnitude of the heat flow to the substrate during τ_{fa} if no heat was being transported simultaneously through the air. This latter term was subtracted from the total heat to be removed during freezing, and τ_{fa} was recalculated for this reduced requirement. This process was repeated until the sequence of freezing times so calculated converged, to an acceptable degree of accuracy.

It is interesting to note that when ventilation is taken into account, as is appropriate both for our experiments and for droplets freezing onto soft hailstones in natural clouds, the heat loss to the air by conduction and evaporation cannot be ignored, as it usually has been. We calculate, for example, that at $-20°C$, in the conditions existing in our experiments, the heat loss to the air is roughly equal to that to the substrate. At significantly higher temperatures, transfer to the air becomes the dominant mechanism of heat loss.

Thus, as T increases, it becomes more probable that during the process of freezing a closed ice shell surrounding a liquid interior will be formed, resulting in the development of great pressures inside the droplet, and its subsequent shattering or splintering. This argument may have some bearing on the observation by Hallett and Mossop (1974) that their mechanism of ice crystal production by droplet accretion onto soft hailstones, is confined to a temperature band close to 0°C.

Since the diffusivity of water vapour in air is approximately equal to the thermal diffusivity in air, the ventilation coefficients for vapour diffusion and the heat conduction will be approximately the same. The latter can be determined experimentally for an object of any shape by measuring the change in temperature or alternatively the heat losses at constant temperature—with and without ventilation. Such tests were performed for the 5 mm diameter rod employed in our primary experiments. A value of $f = 15 \pm 3$ was determined and used in the droplet freezing time calculation.

REFERENCES

Brook, M. 1958 *Recent advances in thunderstorm electricity*. Pergamon Press, New York

Buser, O and Aufdermaur, A. N. 1977 'Electrification by collision of ice particles on ice or metal targets'. In *Electrical processes in atmospheres*. Steinkopf, Darmstadt

Caranti, J. M. and Illingworth, A. J. 1980 Surface potentials of ice and thunderstorm charge separation. *Nature*, **284**, 44–46

Carslaw, H. S. and Jaeger, J. C. 1959 *Conduction of heat in solids*. Clarendon Press

Chisnell, R. F. and Latham, J. 1976 Ice particle multiplication in cumulus and clouds. *Q. J. R. Meteorol. Soc.*, **102**, 133–156

Christian, H., Holmes, C. R., Bullock, J. W., Gaskell, W., Illingworth, A. J. and Latham, J. 1980 Airborne and ground-based studies of thunderstorms in the vicinity of Langmuir Laboratory. *ibid.*, **106**, 159–174

Dye, J. E., Jones, J. J., Winn, W. P., Cerni, T. A., Gardiner, B. A., Lamb, D., Pitter, R. L., Hallett, J. and Saunders, C. P. R. 1986 Early electrification and precipitation development in a small, isolated Montana cumulonimbus. *J. Geophys. Res.*, **91**, 1231–1247

Fletcher, N. H. 1962 *The physics of rainclouds*. C.U.P.

Gaskell, W. and Illingworth, A. J. 1980 Charge transfer accompanying individual collisions between ice particles and its role in thunderstorm electrification. *Q. J. R. Meteorol. Soc.*, **106,** 841–854

Gaskell, W., Illingworth, A. J., Latham, J. and Moore, C. B. 1978 Airborne studies of electric fields and the charge and size of precipitation elements in thunderstorms. *ibid.*, **104,** 447–460

Hallett, J. and Mossop, S. C. 1974 The production of secondary ice particles during the riming process. *Nature*, **249,** 26

Hallett, J. and Saunders, C. P. R. 1979 Charge separation associated with secondary ice crystal production. *J. Atmos. Sci.*, **36,** 2230–2235

Illingworth, A. J. 1985 Charge separation in thunderstorms: Small scale processes. *J. Geophys. Res.*, **90,** 6026–6032

Illingworth, A. J. and Latham, J. 1977 Calculations of electric field growth field structure and charge distributions in thunderstorms. *Q. J. R. Meteorol. Soc.*, **103,** 281–295

Jayaratne, E. R. 1981 'Laboratory studies of thunderstorm electrification'. Ph.D. thesis, Manchester

Jayaratne, E. R. and Saunders, C. P. R. 1985 Thunderstorm electrification: The effect of cloud droplets. *J. Geophys. Res.*, **90,** 13063–13066

Jayaratne, E. R., Saunders, C. P. R. and Hallett, J. 1983 Laboratory studies of the charging of soft-hail during ice crystal interactions. *Q. J. R. Meteorol. Soc.*, **109,** 609–630

Krehbiel, P. R., Brook, M. and McCrory, R. A. 1979 An analysis of the charge structure of lightning discharges to ground. *J. Geophys. Res.*, **84,** 2432–2456

Krehbiel, P. R., Brook, M., Lhermitte, R. L. and Lennon, C. L. 1983 'Lightning charge structure in thunderstorms'. Pp. 408–411 in *Processes in atmospheric electricity*. Eds. L. H. Ruhnke and J. Latham. Deepak

Latham, J. 1981 The electrification of thunderstorms. *Q. J. R. Meteorol. Soc.*, **107,** 277–298

Latham, J. and Mason, B. J. 1961 Electric charge transfer associated with temperature gradients in ice. *Proc. R. Soc. London*, **A260,** 523–536

Lhermitte, R. and Krehbiel, P. R. 1979 Doppler radar and radio observations of thunderstorms. *IEE Trans. Geosci-Electronics*, **GE17,** 162–171

Macklin, W. C. and Payne, G. S. 1967 A theoretical investigation of the ice accretion process. *Q. J. R. Meteorol. Soc.*, **93,** 195–214

Mossop, S. C. 1984 Production of laboratory clouds. *ibid.*, **110,** 275–279

Orville, R. E. 1987 Meteorological applications of lightning data. *Rev. Geophys.*, **25,** 411–414

Pruppacher, H. R. and Klett, J. D. 1978 *Microphysics of clouds and precipitation.* D. Reidel. Pub. Co.

Rawlins, F. 1982 A numerical study of thunderstorm electrification using a three-dimensional model incorporating the ice phase. *Q. J. R. Meteorol. Soc.*, **108,** 779–800

Reynolds, S. E., Brook, M. and Gourley, M. F. 1957 Thunderstorm charge separation. *J. Meteorol.*, **14,** 426–436

Takahashi, T. 1978 Riming electrification as a charge generation mechanism in thunderstorms. *J. Atmos. Sci.*, **35,** 1536–1548

Workman, E. J. and Reynolds, S. E. 1948 A suggested mechanism for the generation of thunderstorm electricity. *Phys. Rev.*, **74,** 709